A Direct Optimal Control Strategy for Valves in Heat Exchanger Networks and Experimental Validations

Yi-Fei Wang, Qun Chen *

Tsinghua University, Beijing, China, chenqun@tsinghua.edu.cn

1. Abstract

Optimal operations of heat exchanger networks (HENs) are of great significance to energy conservation. As one of the most efficient methods to reduce the running costs of HENs, the pressure differential set points control strategy has been widely applied in practice, where the optimal pressure differentials of different sections are obtained by suitable empirical and mathematical models, and then the optimal pressure differentials are passed to control systems to guide the operations of each component. Most control systems in these methods are indirect control strategies. That is, it will take a long time to seek the operating parameters of each component due to the lack of direct operating parameters. Based on the newly proposed thermal resistance-based optimization method, we introduce a direct optimal control strategy for adjustable valves in HENs to obtain the optimal valve openings directly with the full awareness of HENs in physics. Finally, we take a variable water volume chiller system as an example to validate the proposed control strategy. Groups of experiments and the results illustrate the proposed direct valve control strategy of the HEN.

2. Keywords: heat exchanger networks; energy conservation; valve opening; control strategy.

3. Introduction

Heat exchanger networks (HENs) take the main components and cost large proportion of energy consumption in many engineering fields, such as power plant and chemical industries. Energy conservations demands the optimizations of HENs, where adjustable valve is an efficient way for HENs optimal control [1].

The main control method of adjustable valve focuses on the pressure differential set points control strategy. For instance, Wang et al. [2] proposed a pressure set point control method for an indirect water-cooled chilling system, and Lu et al. [3] raised a optimization method for a heat, ventilation and air condition (HVAC) system with the duct differential pressure set point. Besides, pressure differential of other set points also work in the optimal operating of HENS, such as the pressure differential of secondary VSP [4, 5], the fan static pressure [6], and the pressure drop through the heat exchanger [2].

However, the direct control parameters in a HEN are the opening of valves, rather than the set points of pressure differentials. With these optimal set points, it is unavoidable to control the valve openness by seeking the help of some control strategies, such as the PID controllers [3, 4, 7], the direct digital control (DDC) strategies [8], the online control strategies [9], and the feedback [10] or self-turning control strategies [11, 12].

Actually, the aforementioned methods with the optimal set points and the control strategies divide the optimization into two sequential steps virtually. One is to get the optimal set points to satisfy the requirements, and the other is to achieve these set points by regulating the valves through control strategies. However, these two sequential steps separate the influences of the valves and pipelines characteristics out of the global system performance, and consequently narrow down the range of the optimization results artificially. What's more, the control strategies require more or less setting time [13, 14]. The set points are only controlled close to but not indeed the optimal values, and incessantly varied within a range, which is influenced by the controller [15, 16].

In order to directly obtain the optimal valve openness for each pipeline, Chen et al. [17] provide a thermal resistance-based method for HEN optimization, which links the operating parameters, i.e. the valve openness, directly to the requirements, such as the required heat transfer rate and the surrounding temperature, and the performance of each component, including the heat exchanger thermal conductances, the pump characteristics, and the pipeline characteristics.

This paper provides an effort to obtain the direct optimal openness of the adjustable valves for HEN optimizations, avoiding the inconvenient control strategies with intermediate set points values. Based on the physical models of heat exchangers, pumps, and pipelines, we first fit the thermal conductances of heat exchangers and the characteristic parameters of pumps and pipelines in a VWV HEN by a series of experiments. With these fitted physical models, utilization of the thermal resistance-based optimization method directly offers different optimal valve openness under different operating conditions. Experimental measurements of the HEN performance illustrate that the optimized valve openness indeed lead to the lowest total energy consumptions of the HEN under different operating conditions.

4. Experiment facilities and measurement instruments

Fig.1 gives the sketch and the photo of an experimental HEN studied in this paper, consisting of two counter-flow plate heat exchangers, three adjustable valves (AV), three variable speed pumps (VSP), a thermostatic hot water tank, a chiller, and pipelines wrapped up with thermal insulating materials. The working fluids in Loop 1 and 3 are water, and that in Loop 2 is a refrigerant R142b. The pumps drive the working fluids to circulate in each loop, transferring heat in the thermostatic hot water tank through heat exchanger 1, heat exchanger 2, finally to the evaporator of the chiller. Three turbine volume flow-meters (VFM) with an accuracy ±0.5% of the full scale 20 L/min are utilized to measure the fluid flow rates in three loops. Three differential pressure transducers (DPT) with an accuracy ±0.2% of the full scale 350 kPa are employed to measure the pressure differentials of each VSP. A pressure gauge (PG) with the full scale 1.8 Mpa is equipped in Loop 2 to monitor the refrigerant absolute pressure. T type copper-constantan thermocouples (Produced by Omega Engineering) with an accuracy ±0.2 ^{o}C serve to test the working fluid temperatures in each measurement points shown in Fig.1, where two thermocouples are placed in each point for accuracy. The subscript w and r represent water and refrigerant, i and o mean the inlet and the outlet of heat exchangers, and 1, 2 and e stand for heat exchanger 1, heat exchanger 2 and the evaporator, respectively. In addition to the measuring instruments, the experiment system also contains a data acquisition and control system (DACS) to log the measured data, including volume flow rates, pressure differentials and temperatures, and control the components, such as the openness of the AVs and the water temperature of the tank.
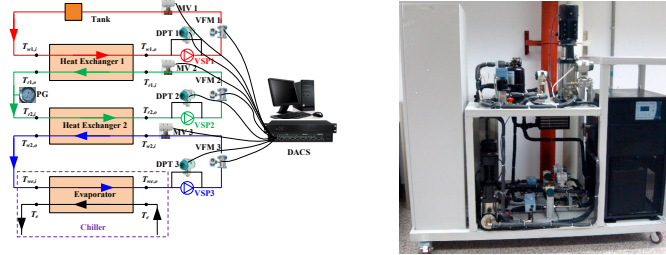
Fig.1 The sketch of a variable water volume heat exchanger network and the photo of the experiment facility

5. Physical models of each component
5.1 Physical models of heat exchangers

For the counter-flow heat exchangers, i.e. heat exchanger 1 and 2, the entransy dissipation-based thermal resistances are [18]

$$R_{hx1} = \frac{(T_{w1,i} + T_{w1,o}) - (T_{r1,i} + T_{r1,o})}{2Q} = \frac{\xi_1}{2} \frac{\exp[(kA)_1 \xi_1] + 1}{\exp[(kA)_1 \xi_1] - 1}, \quad \xi_1 = \frac{1}{m_1 c_{p,1}} - \frac{1}{m_2 c_{p,2}}, \tag{1}$$

$$R_{hx2} = \frac{(T_{r2,i} + T_{r2,o}) - (T_{w2,i} + T_{w2,o})}{2Q} = \frac{\xi_2}{2} \frac{\exp[(kA)_2 \xi_2] + 1}{\exp[(kA)_2 \xi_2] - 1}, \quad \xi_2 = \frac{1}{m_2 c_{p,2}} - \frac{1}{m_3 c_{p,3}}, \tag{2}$$

where R is the entransy dissipation-based thermal resistance, ξ is the flow arrangement factor of a heat exchanger, k is the heat transfer coefficient, A is the heat transfer area, m is the mass flow rate, and c_p is the constant pressure specific heat. The subscripts $hx1$ and $hx2$ represent heat exchangers 1 and 2, and the numbers 1, 2, and 3 represents the liquid driven by the pump$_1$, pump$_2$, and pump$_3$, respectively.

By assuming the evaporation temperature constant, the physical model of the evaporator is [18]

$$R_e = \frac{T_{we,i} + T_{we,o} - 2T_e}{2Q} = \frac{\xi_e}{2} \frac{\exp[(kA)_e \xi_e] + 1}{\exp[(kA)_e \xi_e] - 1}, \quad \xi_e = \frac{1}{m_3 c_{p,3}}, \tag{3}$$

where the subscript e stands for the evaporator.

Similarly, the entransy dissipation-based thermal resistance for the mixing process of the cooled hot water and the tank water gives [18]

$$R_m = \frac{T_{w1,i} - T_{w1,o}}{2Q} = \frac{1}{2m_1 c_{p,1}}, \tag{4}$$

where the subscript m means the mixing process.

5.2 Physical models of pumps

For a pump operating in a given speed, the mass flow rate m, and the head loss or the pressure drop H obey the following formula [19, 20]

$$H = a_0 + a_1 \frac{m}{\rho} + a_2 \frac{m^2}{\rho^2}, \tag{5}$$

where a_0, a_1, a_2 are the characteristic parameters of pump, which can be identified by experimental data, and ρ is the working fluid density.

Without considering the mechanical losses, the power consumption of the pump is represented as

$$P = mgH .\tag{6}$$

5.3 Physical models of pipelines with an adjustable valve in different openness

The head loss or the pressure drop of the pipelines with an adjustable valve in different openness, is calculated by [21]

$$H = H_s + H_d + H_v ,\tag{7}$$

where H_s is the static head that the pump needs to lift, H_d is the dynamic head, and H_v is the head loss caused by the adjustable valve.

The dynamics head of the pump is expressed by [22]

$$H_d = dm^2, d = \frac{1}{2g\rho^2 S^2}\left(\frac{fL}{D} + \sum K_i\right),\tag{8}$$

where f is the Darcy friction-factor, L is the length of pipe, D is the pipe diameter, and K is the minor loss coefficient of the detail structure.

Assuming the valve openness in the given pipeline is c, the additional head loss caused by the valve, i.e. H_v, can be seen as a sudden contraction expressed as [22]

$$H_v = \left[b_1\left(1-c\right)^2 + b_2\left(1-c\right)\right]m^2 .\tag{9}$$

where b_1 and b_2 are the coefficients, which are related to the size of the valve and the pipelines.

Then the pipeline head loss with a valve openness being c follows

$$H = H_s + \left[d + b_1\left(1-c\right)^2 + b_2\left(1-c\right)\right]m^2 .\tag{10}$$

6. Determination of the characteristic parameters of each component

In order to identify the thermal conductances of heat exchangers, the characteristic parameters, a_0, a_1 and a_2 in Eq. (6), of pumps, and the characteristic parameters, H_s, b_1, b_2, and d in Eq. (12), of pipelines, a group of experiments are conducted. In the experiments, the proprieties of water and R142b are assumed constant. The water average density is 1000 kg/m^3, and the water constant pressure specific heats is 4196 J/(kg K). The absolute pressure of Loop 2 is 0.47 MPa. In this condition, by referring to NIST-Refprop, the average density of R142b is 1100 kg/m^3, and the constant pressure specific heat is 1304 J/(kg K). (300 K ± 10 K, saturated liquid).

6.1 Experiment to determine the thermal conductances of heat exchangers

We set the operating frequencies of pump$_1$, pump$_2$, and pump$_3$ at 30, 40 and 20 Hz, respectively, the temperature difference of the thermostatic hot water tank and the evaporating temperature is kept as 40 ^{o}C. Under this working condition, we operate the experiment system at steady-state condition for 30 minutes, which are monitored by the DACS. Table 1 offers the thermal conductances of all heat exchangers in this operating condition.

Table 1 The thermal conductances of each heat exchanger

kA	$(kA)_1$	$(kA)_2$	$(kA)_3$
Value(W/K)	219.3	196.7	53.2

Because the thermal conductances are influenced by the fluid velocities, it is need to re-calculate the thermal conductances case by case with different working parameters.

6.2 Experiments to identify the characteristic parameters of pumps

The working point of each pump is determined by the mass flow rate and the head loss with the relation given in Eq. (5). We preform experiments with the three pumps at given rotation speeds, i.e. 30 Hz, 40 Hz and 20 Hz, respectively, and change the opening of the adjustable valves at 100%, 80%, 60%, 50%, 40%, 30% and 20%, sequentially. The average mass flow rates, the head losses of each pump and the fitted m-H curves are given in Fig.2. The points exp_1, exp_2, and exp_3 represent the experiment data, and the dash lines fit_1, fit_2, and fit_3 stand for the fitted m-H curves, respectively. Table 2 exhibits the characteristic parameters of the pumps and the maximum deviations between the experimental data and the fitted values, δ_{max}.
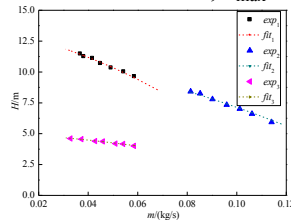
Fig. 2 The experiment data and the fitted curves of each pump at given speed

Table 2 The characteristic parameters of pump s and the maximum deviations

Pump	a_0	a_1	a_2	δ_{max}
pump$_1$	13.4	-32.6	-567.4	0.55%
pump$_2$	5.1	-9.8	-141.5	3.73%
pump$_3$	11.6	-18.5	-261.2	1.29%

The maximum deviations between the experiment data and the calculated values of pump$_1$, pump$_2$, and pump$_3$ are 5.31%, 4.95% and 5.17%, in sequence.

6.3 Experiments to identify the characteristic parameters of pipelines with different valve openness

For identifying the characteristic parameters, i.e. H_s, b_1, b_2, and d. We conduct experiments at 100 %, 50 %, 75 %, 25 % opening of the adjustable valve and with the valve openness of the VSPs at 50 Hz, 45 Hz, 40 Hz, 35 Hz, 30 Hz, 25 Hz and 20 Hz, sequentially. Fig.3 offers the averaged mass flow rates, the head losses of each pipeline and the fitted or calculated *m-H* curves of each pipeline, respectively, where the subscript *exp* means experimental values, *fit* represents the fitted values, and *cal* stands for the calculated values. Table 3 lists the characteristic parameters of the pipelines, and the maximum deviations between the experiment data and the fitted values.
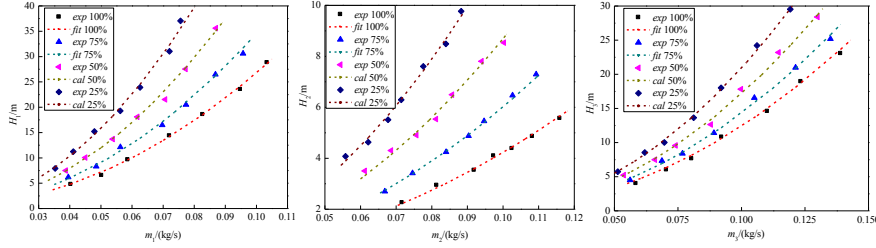
Fig. 3 The experiment data and the fitted curves of Loop 1 at different opening of the adjustable valve

Table 3 The characteristic parameters of pipelines and the maximum deviations

Parameter	H_s	d	b_1	b_2	δ_{max}
Loop 1	0.569	2623.55	3099.3	2327.3	0.55%
Loop 2	0.358	1205.17	757.3	567.9	3.73%
Loop 3	0.1	413.04	711.4	536.0	1.29%

7. The thermal resistance-based method for HEN optimization

Based on the physical models of heat exchangers in Part 3.1, combining Eqs. (1) ~ (4) offers the inherent relation of the heat transfer processes in the entire experiment system [17, 18]:

$$T_h - T_e = Q\left(R_m + R_{hx1} + R_{hx2} + R_e\right). \tag{11}$$

For a VWV HEN with given pipeline structures, pumps, valves and heat exchangers, it is always needed to seek the optimal operating parameters of each valve for such objective as the minimum total power consumption of all pumps, at a fixed heat transfer rate, which is relevant to the running cost. With the power consumption of a pump given in Eq. (6), ignoring the mechanical losses, the total one of all pumps is

$$P_t = \sum_i P_i = \sum_i m_i g H_i. \tag{12}$$

The optimization for minimizing the total power consumption of all pumps, with the constraints expressed in Eqs. (5), (10) and (11), can be converted as a conditional extremum problem by the method of Lagrange multipliers, which provides a Lagrange function as

$$\Pi = \sum_i P_i + \alpha\left[T_h - T_e - Q\left(R_m + R_{hx1} + R_{hx2} + R_e\right)\right]$$
$$+ \gamma_i\left[H_{s,i} + d_i m_i^2 + b_{1,i}\left(1 - c_i\right)^2 m_i^2 + b_{2,i}\left(1 - c_i\right)m_i^2 - H_i\right], \tag{13}$$
$$+ \beta_i\left(a_{0,i} + a_{1,i}\frac{m_i}{\rho_i} + a_{2,i}\frac{m_i^2}{\rho_i^2} - H_i\right) \qquad i = 1, 2, 3$$

where α, β and γ are the Lagrange multiplies.

Making the partial derivations of the Lagrange function with respect to m_i, c_i, and H_i equal to zero offers the optimization equation set. Solving the equation set and Eqs. (5), (10), (11) simultaneously will get the optimal values of all the unknown parameters, including the openness of the adjustable valves, for the minimum total power consumption.

8. Experimental results and discussions

Based on the optimal openness of the adjustable valves for the given heat transfer rate and the referenced thermal conductances, we operate the experiment system at steady-state for 30 minutes. The DACS records temperatures and volume flow rates of each measurement point, and averaged values can be obtained. Since the thermal

conductance varies with different fluid velocities, it is necessary to compare the actual thermal conductances to the referenced ones during optimization, to ensure these valve openness being the optimal ones by eliminating the influences to the thermal conductances from different fluid velocities. If the thermal conductances deviations between experimental values and the referenced ones are within 5%, which is thought as the measurement uncertainties, experiment in that case is regarded as the one with optimal openness of the adjustable valves. Otherwise, optimization calculations should be made again with the newly experimental thermal conductances values, until deviations are within 5%. Obviously, the heat transfer rates by the experiment should be near the given heat transfer ones within the measurement uncertainties. To make it clear, the flowchart of this procedure is as below
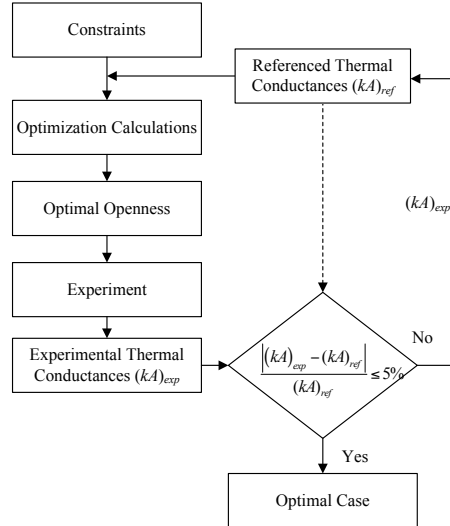
Fig.4 The flowchart of the optimization procedure used for finding actual optimal cases

8.1 Experiments with the optimal valve openness

When the heat transfer rate is fixed at 1000 W, and the temperature difference of the thermostatic hot water tank and the evaporating temperature is kept as 40 $^{\circ}$C, solving Eqs. (5), (10), (11), and the equation set from the Lagrange function gives the optimal valve openness with the lowest total power consumption.. Table 4 exhibits the average temperatures at each measurement point, and the average volume flow rates and the corresponding mass flow rates in each loop with the optimal valve openness.

Table 4 The optimal valve openness of the adjustable valves

Openness	c_1	c_2	c_3
Value (100%)	53%	56%	45%

The average heat transfer rate is 1016 W. The maximum deviation to the average value is 1.28% from heat exchanger 1 (1003 W), and the maximum deviation to the target value 1000 W is 2.70% from evaporator, which are within the measurement uncertainties. Table 5 provides the experimental results of the head losses, the power consumptions of each pump and the corresponding total power consumption of all the pumps.

Table 5 The experimental results of the head losses, the power consumptions of each pump and the corresponding total power consumption of all the pumps

Parameter	H_1(m)	H_2(m)	H_3(m)	P_1(W)	P_2(W)	P_3(W)	P_t(W)
Experiment value (W/K)	10.57	7.38	4.36	4.95	6.98	1.89	13.82

8.2 Experiments with other alternative operating frequencies

Alternative experiments with the valve openness listed in Table 6 can also satisfy the same requirements, i.e. the heat transfer rate 1000 W, the temperature difference of the thermostatic hot water tank and the evaporating temperature 40 $^{\circ}$C. Table 7 offers the energy consumptions of all the pumps in different alternative experiments.

Table 6 The valve openness of the adjustable valves in different alternative experiments

Openness (100%)	No.1	No.2	No.3	No.4	No.5	No.6	No.7
c_1	47%	48%	49%	50%	52%	51%	54%
c_2	60%	59%	57%	56%	55%	58%	56%
c_3	48%	52%	54%	55%	50%	54%	57%

Table 7 The energy consumptions of all the pumps in each alternative experiment

Case	No.0	No.1	No.2	No.3	No.4	No.5	No.6	No.7
Value(W)	13.82	15.50	14.99	15.03	15.04	14.87	15.29	15.47

It is shown in Table 7 that the power consumption of the optimized operating condition is lower than those of any other alternative ones, which validate our newly proposed optimal control strategy for HENs.

9. Conclusions

Based on the physical models of such components as heat exchangers, pumps and pipelines with adjustable valves in a HEN, we determined the characteristic parameters in these models for specific components experimentally. Combination of these physical models and the newly proposed thermal resistance-based optimization method for HENs offered a direct valve openness control strategy, which directly control the operation of a HEN with certain system requirements and constraints, such as prescribed heat transfer rates, fixed structures of heat exchangers and pipelines.

Further experimental results with the optimal valve openness and other alternative ones under the same system requirements showed that the total power consumption of all pumps in the optimal experiment was actually the lowest one, which validated our newly proposed direct optimal control strategy.

Reference

[1] M. Bojic, N. Trifunovic, Linear programming optimization of heat distribution in a district-heating system by valve adjustments and substation retrofit, *Build Environ*, **35** (2000) 151-159.

[2] S.W. Wang, J. Burnett, Online adaptive control for optimizing variable-speed pumps of indirect water-cooled chilling systems, *Appl Therm Eng*, **21** (2001) 1083-1103.

[3] L. Lu, W.J. Cai, L.H. Xie, S.J. Li, Y.C. Soh, HVAC system optimization - in-building section, *Energ Buildings*, **37** (2005) 11-22.

[4] X.Q. Jin, Z.M. Du, X.K. Xiao, Energy evaluation of optimal control strategies for central VWV chiller systems, *Appl Therm Eng*, **27** (2007) 934-941.

[5] Z.J. Ma, S.W. Wang, Energy efficient control of variable speed pumps in complex building central air-conditioning systems, *Energ Buildings*, **41** (2009) 197-205.

[6] M. Ning, M. Zaheeruddin, Neuro-optimal operation of a variable air volume HVAC&R system, *Appl Therm Eng*, **30** (2010) 385-399.

[7] J. Sun, A. Reddy, Optimal control of building HVAC&R systems using complete simulation-based sequential quadratic programming (CSB-SQP), *Build Environ*, **40** (2005) 657-669.

[8] D.L. Loveday, G.S. Virk, Artificial-Intelligence for Buildings, *Appl Energ*, **41** (1992) 201-221.

[9] Z.J. Ma, S.W. Wang, F. Xiao, Online performance evaluation of alternative control strategies for building cooling water systems prior to in situ implementation, *Appl Energ*, **86** (2009) 712-721.

[10] X.Y. You, X. Xiao, Active control of laminar stability by feedback control strategy, *Int J Heat Mass Tran*, **43** (2000) 3529-3538.

[11] H.B. Duan, Y. Fan, L. Zhu, What's the most cost-effective policy of CO2 targeted reduction: An application of aggregated economic technological model with CCS?, *Appl Energ*, **112** (2013) 866-875.

[12] H. Miki, A. Shimizu, Dynamic characteristics of phosphoric-acid fuel-cell stack cooling system, *Appl Energ*, **61** (1998) 41-56.

[13] G.F. Franklin, J.D. Powell, A. Emami-Naeini, Feedback Control of Dynamic Systems, 4th ed., Addison Wesley, New Jersey, USA, 1993.

[14] K. Ogata, Modern Control Engineering, 4th ed., Prentice Hall, New Jersey, USA, 2010.

[15] B.C. Kuo, F. Golnaraghi, Automatic Control Systems, 8th ed., Wiley, New Jersey, USA, 2002.

[16] G.F. Franklin, J.D. Powell, M.L. Workman, Digital Control of Dynamic Systems, 3rd ed., Prentice Hall, New Jersey, USA, 1997.

[17] Q. Chen, Y.-F. Wang, Y.-C. Xu, A thermal resistance-based method for the optimal design of central variable water/air volume chiller systems, *Appl Energ*, **139** (2015) 119-130.

[18] Q. Chen, Entransy dissipation-based thermal resistance method for heat exchanger performance design and optimization, *Int J Heat Mass Tran*, **60** (2013) 156-162.

[19] Z.Y. Yang, H. Borsting, Energy Efficient Control of a Boosting System with Multiple Variable-Speed Pumps in Parallel, *Ieee Decis Contr P*, (2010) 2198-2203.

[20] Z.Y. Yang, H. Borsting, Optimal Scheduling and Control of a Multi-Pump Boosting System, *Ieee Intl Conf Contr*, (2010) 2071-2076.

[21] J.B. Rishel, HVAC pump handbook, McGraw-Hill, New York, USA, 1996.

[22] W.F. M., Fluid mechanics, 4th ed., WCB/McGraw-Hill, Mass, USA, 1999.